ARCHIVES
of
FOUNDRY ENGINEERING

ISSN (2299-2944)
Volume 2025
Issue 4/2025

155 – 161

10.24425/afe.2025.157613

20/4

Published quarterly as the organ of the Foundry Commission of the Polish Academy of Sciences

Effect of Titanium on Structural, Mechanical and Functional Properties of Thin-Walled CGI Castings

M. Kawalec [a, *], M. Górny [a], J. Kozana [b], J. Marosz [a]
[a] AGH University of Science and Technology in Kraków
Faculty of Foundry, Department of Alloy and Composite Engineering, Poland
[b] AGH University of Science and Technology in Kraków, Faculty of Foundry
Department of Molding Materials, Mold Technology, and Non-Ferrous Metal Foundry
* Corresponding author: E-mail address: kawalec@agh.edu.pl

Received 18.07.25; accepted in revised form 31.10.25; available online 31.12.2025

Abstract

This study investigates the impact of titanium (Ti) additions, up to 0.13 wt%, on the microstructure and mechanical properties of iron castings. To account for varying cooling rates, the research examined thin-walled castings with thicknesses of 3 mm and 5 mm, alongside a 13 mm thick reference casting.
Microstructural changes were quantitatively assessed using image analysis and qualitatively examined with a scanning electron microscope (SEM). The addition of 0.13% Ti was found to significantly influence graphite formation in thin-walled castings, reducing the graphite nodule fraction in 3 mm castings from 73% to 34%. In 5 mm castings, the nodule fraction was reduced to below 20%, meeting ASTM standards. The study also measured key mechanical and functional properties, including hardness, wear resistance, and machinability. While hardness showed no significant increase with Ti additions, the ultimate tensile strength of 5 mm castings with 0.10% Ti increased slightly before decreasing with higher Ti content.
Metallographic analysis revealed that the addition of titanium significantly influences graphite formation in thin-walled castings, to a much greater extent than in thicker sections. This is particularly crucial given the differing solidification kinetics in components of varying thicknesses. Furthermore, thin-walled castings with a high degree of inoculation that solidified under high cooling rates exhibited a homogeneous structure, free from chilling. This desirable microstructure, combined with favorable mechanical and functional properties, positions these castings for potential use as substitutes for aluminum alloy castings in diverse applications.

Keywords: Innovative foundry technologies and materials, Metallography, Compacted graphite, Titanium, Thin wall castings

1. Introduction

Compacted Graphite Iron (CGI), also known as vermicular graphite cast iron, has emerged as a material of significant interest across various industries, particularly in the automotive sector [1-4]. Its attractive features, such as excellent vibration damping capacity, good thermal conductivity, and the ability to withstand higher pressures, make it a preferred alternative to traditional grey cast iron in components like brake discs, brake drums, exhaust manifolds, engine heads, and diesel engine blocks [5,6]. The use of CGI in diesel engines notably enhances combustion efficiency and overall performance. Furthermore, from an economic and ecological perspective, thin-walled CGI castings present a

compelling alternative to lightweight aluminum alloy castings, offering competitive mechanical properties at a relatively lower production cost [7].

The complex microstructure of CGI castings is primarily governed by several critical factors, including chemical composition, cooling rate, liquid treatment, and subsequent heat treatment [8,9]. The cooling rate, a crucial parameter, is intrinsically linked to the casting's section size, pouring temperature, and the thermal properties of the mold material. Producing thin-walled castings presents unique challenges due to the wide range of cooling rates experienced during the initial stages of graphite eutectic solidification [10]. As the cooling rate increases in these thin sections, the extent of thermal undercooling also rises, leading to a progressive shift in graphite morphology towards a more nodular form. This results in an increased nodule count and a reduced compacted graphite ratio, making the manufacturing of thin-walled compacted iron castings considerably more complex than that of thicker sections [11]. Recent research by [12] further elaborates on the intricate relationship between cooling rate and graphite morphology in thin-walled castings, highlighting the criticality of process control. Similarly, [13] provides an in-depth analysis of solidification behavior in such challenging geometries, underscored by the need for precise parameter management.

Controlling the formation of CGI is notoriously difficult, primarily due to the narrow permissible range of residual magnesium (Mg). An excess of Mg can lead to an undesirable proliferation of graphite nodules, while an insufficient amount can result in the formation of flake graphite, characteristic of grey iron [14]. Even at magnesium levels as low as 0.01%, achieving acceptable CGI in sections with wall thicknesses of 4 mm or less can be challenging due to excessive graphite nodularity [7]. To circumvent these limitations, industrial practice often incorporates anti-spheroidizing elements such as aluminum (Al), bismuth (Bi), titanium (Ti), zirconium (Zr), and antimony (Sb) [8,9]. Among these, titanium (Ti) is a key alloying element that offers distinct advantages, particularly when combined with magnesium, as it extends the effective working range of magnesium, facilitating the consistent production of CGI castings [8,9]. However, the use of titanium is not without its drawbacks, including potential contamination of casting returns and a reduction in machinability [1]. Despite diligent foundry practices and strict production discipline, maintaining the desired microstructure consistency without the judicious use of anti-spheroidizing elements like titanium remains challenging. While existing literature provides some insights [1,7,15], there is a notable gap in comprehensive data concerning the specific influence of Ti addition on the high cooling rate-structure relationships in CGI, a property of paramount importance for the successful fabrication of thin-walled castings. This article aims to address this gap by presenting a detailed analysis of the impact of Ti addition on the microstructure and mechanical properties of thin-walled CGI castings with varying wall thicknesses. Recent work by [16] has explored the role of Ti in controlling graphite morphology in similar systems, providing a valuable context for the current study. Furthermore, recent advancements in CGI technology, as discussed by [17] regarding thermal conductivity and by [18] concerning mechanical properties under varying cooling conditions, emphasize the ongoing relevance of this research. The comprehensive review of graphite morphology control in CGI by [19] and the detailed study on the influence of inoculation on thin-walled castings by [20] offer additional crucial context for understanding the complexities involved.

2. Experimental

The experimental melts were conducted in a 15 kg capacity, intermediate-frequency electric induction furnace. The furnace charge comprised Sorelmetal, technically pure silicon, Fe-Mn, Fe-S, and steel scrap. Following heating of the metal to 1490°C, the melt was held for 2 minutes. The target chemical composition for the melts was as follows: carbon (C) in the range of 3.60 - 3.70 wt%, silicon (Si) from 2.40-2.60 wt%, manganese (Mn) from 0.03-0.05 wt%, sulfur (S) from 0.01-0.02 wt%, and magnesium (Mg) from 0.01-0.02 wt%. The titanium content was 0.01 wt% in heat No. I, 0.10 wt% in heat No. II, and 0.13 wt% in heat No. III.

Vermicularization and inoculation operations were performed using the bell method. For vermicularization, a Fe-Si-Mg foundry alloy (44-48% Si; 5.5-6.2% Mg; 0.8-1.2% RE; 0.8-1.2% Ca; Max. 1%Al; granulation 2-10 mm) and Fe-Ti (70% Ti) were utilized, with quantities as detailed in Table 1. Inoculation was carried out with a Fe-Si alloy inoculant (73-78% Si; 0.75-1.25% Ca; 0.75-1.25% Ba; 0.75-1.25% Al; granulation 1-3 mm) at an addition rate of 0.6 wt. %. The pouring temperature for all melts was 1400°C.

Table 1.
Quantity of vermicularizing agent and Fe-Ti

Heat No.	Vermicularising agent wt. %	Fe-Ti wt. %
I	0.5	-
II	0.7	0.20
III	0.7	0.40

In this experiment, compacted graphite iron (CGI) plate castings with section sizes (G) of 3 mm, 5 mm, and 13 mm were produced to achieve varying cooling rates. Figure 1 shows the method of placing the thermoelement in the mold and presents a schematic of the test block casting. The sand molds were prepared using conventional green molding sand, consisting of silica sand, 7 wt.% bentonite, and a water-to-bentonite ratio of 0.4%. The sand exhibited a granularity range of 100-200 μm.

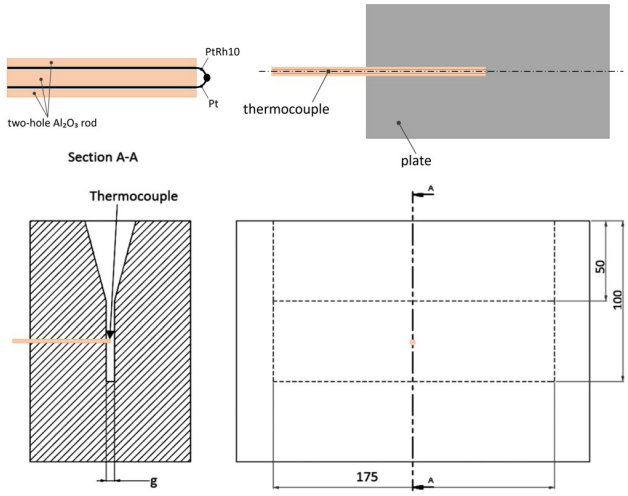

Fig. 1. Schematic of the test block casting with the location of the thermoelement shown

The difference between the amount of Fe-Ti added and the final Ti content in the castings is attributed to the yield of titanium during the melting process. Due to factors such as oxidation and the formation of stable compounds, a portion of the added titanium does not remain in the final alloy. In our heats, this resulted in a Ti yield of approximately 50% for Heat No. II and 32.5% for Heat No. III. The final chemical composition of the castings, as measured after solidification, accurately reflects the effective amount of titanium in the material.

Metallographic characterization was performed using a Leica MEF 4M optical microscope equipped with a QWin v 3.5 quantitative image analyzer, and a Keyence VHX7100 optical microscope. Observations of graphite morphology and matrix were conducted at various magnifications. Additionally, metallographic analysis were examined using a JEOL JSM-550LV scanning electron microscope (SEM) operated at 20 kV.

Brinell hardness, HBW measurements were made in an HPO-250 hardness tester, following the ISO 6506standard and tensile testing (ultimate tensile strength, UTS, 0.2% proof strength, PS0.2 and elongation, A) was performed on flat samples in a universal Zwick/Roell Z050, following the ASTM E8M 6.2 standard. For the mechanical tests, five samples were prepared for each condition. The average value, determined in accordance with the principles of statistical analysis, was treated as the final result and is presented in the work.

Abrasive wear resistance studies were conducted using a Miller machine, following the ASTM G75 standard. Standard specimens, measuring 25.4 x 12.7 x 5 ± 0.9 mm, were loaded with specific weights and subjected to an abrasive wear test. For the abrasion tests, two samples from a single material were tested in each case. This involved rubbing the specimens in a reciprocating motion against the bottom of a gutter filled with an aqueous mixture of an abrasive medium (SiC + distilled water).

The study encompassed three tests, each performed in 16-hour series consisting of four four-hour shifts. Subsequently, the respective wear resistance curves were plotted. After each run, the specimens were washed, dried, and weighed to the nearest 0.1 mg. Based on these measurements, weight losses and cumulative weight losses were determined after each test within a given series, allowing for the results to be plotted on a time-weight graph.

Cumulative (summarized) weight losses, representing the total mass loss since the beginning of constant load application, were recorded after 4, 8, 12, and 16 hours of the test cycle. The obtained changes in specimen weight were approximated by an exponential curve described by the following relationship:

$$W(t) = A \cdot t^{B} \quad (1)$$

where:
W – weight loss, [g],
t – time, [hours],
A, B – constants determined by the least squares method.

Regardless of the number of trials in a series or the duration of a single test, the mass wear rate (V_w) was adopted as the slope of the tangent to the wear curve at the second hour of testing:

$$V_w = A \cdot B \cdot 2^{(B-1)} \quad (2)$$

where:
A, B – constants from relationship (1).

For machinability studies, cutting tools (borer ϕ 5 mm) with identical contours and angles were used, subjected to a force of 500 N. The rotational speed of these tools was 680 revolutions per minute. In each investigated sample, three test holes were bored, and the boring time for each was measured.

3. Experimental results and analysis

3.1. Analysis of microstructure

Metallographic examination revealed a significant effect of titanium (Ti) addition on compacted graphite, particularly in thin-walled castings. The incorporation of Ti necessitates the addition of extra magnesium to safely mitigate the risk of flake graphite formation, as shown in Figure 2.

Studies indicate that Ti addition reduces the graphite nodule fraction in cast iron (3 mm wall thickness) from 73% for the base iron to 34% with the addition of 0.13% Ti. Typically, a limit of 20% nodularity is set for compacted graphite iron (CGI) specifications [8, 9, 12]. For thin-walled castings, CGI naturally tends to solidify with higher nodularity, which can result in outer walls (less than 4-5 mm) exhibiting up to 50% nodularity [1]. However, in the case of thin-walled castings with greater wall thickness (5 mm) and a 0.13% Ti addition, the graphite nodule fraction is reduced to below 20%, thereby meeting ASTM standards [12].

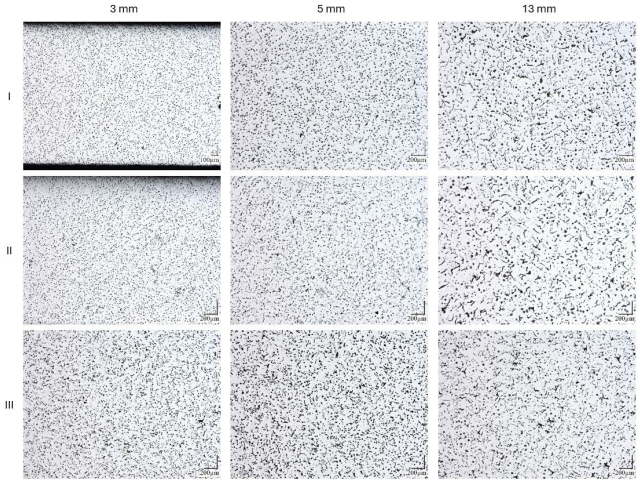

Fig. 2. Microstructures of test block castings with a wall thickness of 3 mm, 5 mm, 13 mm; Mag. 100x. No etchant used

According to the study [15], the addition of 0.15% Ti increases the compacted graphite fraction in castings with a wall thickness of 30-80 mm by only approximately 10%, with a negligible impact on mechanical properties. The present study, however, demonstrates that using 0.13% Ti in thin-walled castings has a much stronger effect on the solidification of compacted graphite compared to castings with thicker sections. Analysis of the cast iron matrix also shows that Ti addition slightly decreases the ferrite fraction in the casting. This is because titanium promotes the solidification of titanium carbides and titanium nitro-carbides within the cast iron microstructure.

The results of metallographic examination are given in Table 2.

Table 2.
The results of metallographic examination

Heat No.	Graphite nodule fraction, %			Ferrite fraction, %			TiC, %
	3 mm	5 mm	13 mm	3 mm	5 mm	13 mm	
I	73	47	20	40	65	90	-
II	46	29	17	40	74	85	< 1
III	34	17	15	30	56	90	< 1

EDS analysis confirmed that the precipitates formed after the introduction of titanium into the cast iron are primarily titanium carbonitrides (Fig. 3a). The stoichiometric form was identified as Ti_2CN, which is consistent with literature data [21, 22]. In addition to carbonitrides, discrete titanium carbide (TiC) precipitates were also observed in the microstructure (Fig. 3b). These titanium carbide inclusions also contained trace amounts of magnesium and sulfur in their chemical composition. Both the titanium carbonitride and titanium carbide precipitates were characterized by their small size, and were homogeneously distributed within both the ferrite grains and the pearlite matrix. While the titanium carbides previously mentioned appeared as faceted crystals, uniformly distributed within the iron matrix, metallographic analysis indicates their maximum size is less than 4 µm, with their volumetric fraction being considerably lower than 1% (Fig. 3).

Producing thin-walled castings presents significant challenges due to the wide range of cooling rates involved. This susceptibility often leads to defects, particularly structural inhomogeneity and the formation of chills [10]. A thorough understanding of how technological factors influence both the cooling rate and the physicochemical state of liquid iron is crucial for manufacturing thin-walled castings with desirable mechanical properties, performance, and minimal casting defects.

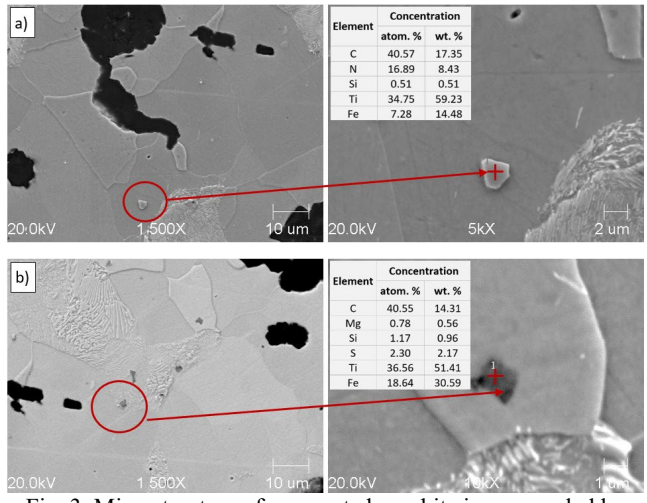

Fig. 3. Microstructure of compacted graphite iron, revealed by scanning electron microscopy (SEM): (a) titanium carbonitride (Ti_2CN); (b) titanium carbide (TiC)

A characteristic feature of thin-walled castings is the significant alteration in cooling rate even with minor variations in wall thickness. Thermal analysis [23] reveals that reducing the wall thickness from 5 mm to 3 mm markedly increases the cooling rate from 10.0°C/s to 26.6°C /s. This accelerated cooling shortens the solidification time from 40 seconds to 18 seconds, elevating the risk of chill formation in cast iron. Consequently, a high degree of inoculation is often required for thin-walled nodular or compacted graphite iron (CGI) castings [13].

However, for CGI, this presents a particular disadvantage: increasing the nucleation potential tends to decrease the amount of compacted graphite while simultaneously increasing the graphite nodule fraction. The present study demonstrates that the addition of titanium (Ti) in highly inoculated thin-walled castings, which solidify under high cooling rates, facilitates the achievement of a homogeneous, chill-free cast iron structure with a high compacted graphite fraction.

3.2. Functional properties

Figure 4, which was developed based on data published in the authors' previous work [23], illustrates the effects of titanium (Ti) addition and casting size on the mechanical properties of compacted graphite iron (CGI) castings.

As shown in Figure 4, there's no significant increase in hardness with Ti additions up to 0.13% (heat No. III). Tensile strength is observed to increase slightly with Ti additions up to 0.10% (heat No. II). However, further increasing the titanium content leads to a decrease in both the tensile strength and the elongation of thin-walled iron castings. This phenomenon is attributed to an increase in the compacted graphite fraction within the cast iron microstructure, characterized by a higher length-to-thickness ratio. For the reference casting (13 mm wall thickness), Ti addition does not appreciably affect the ultimate tensile strength (R_m) or Brinell hardness (HBW), though elongation is reduced to 6.4%.

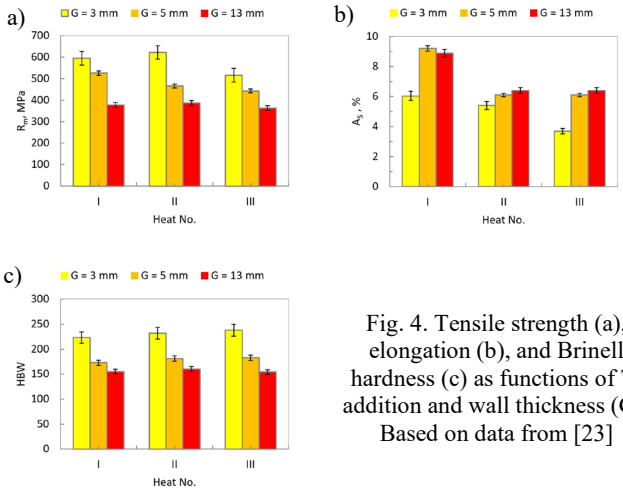

Fig. 4. Tensile strength (a), elongation (b), and Brinell hardness (c) as functions of Ti addition and wall thickness (G). Based on data from [23]

Abrasive wear resistance

To thoroughly evaluate the abrasive wear resistance, tests were conducted using a Miller machine. The investigation focused on heats No. I and III, specifically examining samples with wall thicknesses (G) of 5 mm and 13 mm, respectively. For a broader comparative analysis, additional abrasive wear tests were performed on spheroidal graphite iron (SGI) specimens with a ferritic matrix (F, grade EN-GJS-400-18) and a pearlitic matrix (P, grade EN-GJS-600-3), in accordance with the PN-EN 1563 standard.

Following each test in a given series, precise mass measurements were taken. From these measurements, both individual and cumulative mass losses were meticulously determined. Subsequently, the mass wear rate (V_W) was calculated for each sample, adhering to the methodology outlined in Equation (2). The comprehensive results of these abrasive wear resistance measurements are visually presented in Figure 5.

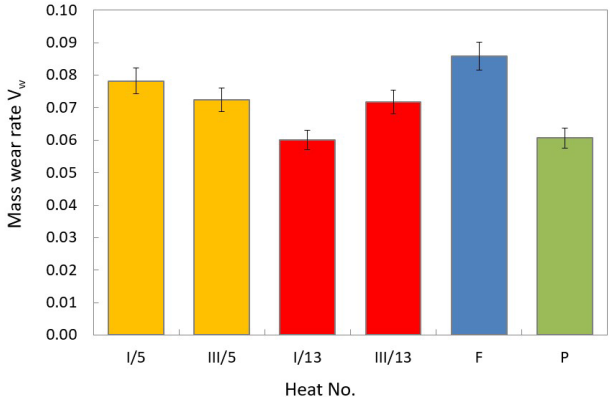

Fig. 5. Results of Abrasive Wear Resistance Measurement
(I/5 – heat No. I, 5 mm wall thickness;
I/13 – heat No. I, 13 mm wall thickness;
III/5 – heat No. III, 5 mm wall thickness;
III/13 – heat No. III, 13 mm wall thickness;
F – spheroidal graphite iron with a ferritic matrix;
P – spheroidal graphite iron with a pearlitic matrix)

Our findings indicate that the addition of titanium (Ti) had a subtle influence on abrasive wear resistance. For samples with a 5 mm wall thickness, a marginal improvement in abrasion resistance was observed. Conversely, for the 13 mm wall thickness, a slight decrease in resistance was noted. It's important to highlight that in both scenarios, these differences were minimal, suggesting a limited direct impact of Ti on overall wear performance within these specific parameters.

When comparing with different matrix structures, all tested samples (those with Ti additions) consistently exhibited slightly lower wear resistance when compared to cast iron with a pearlitic matrix. However, a notable improvement in wear resistance was observed when compared to cast iron with a ferritic matrix. This suggests that while Ti's direct effect on wear was minor, the underlying microstructure played a more significant role in determining the material's ability to resist abrasive forces.

While titanium additions have a minimal direct impact on wear performance, the subtle influence on abrasive wear resistance is primarily attributed to the indirect effects on the matrix and graphite structure. Specifically, the observed titanium carbonitrides (Ti_2CN) and titanium carbides (TiC) are present in very small quantities (volume fraction < 1%) and are finely dispersed. Their limited presence does not significantly alter the overall wear behavior. Instead, the abrasive wear resistance is more prominently influenced by the underlying matrix, with pearlitic structures exhibiting superior wear resistance compared to ferritic ones. The graphite morphology also plays a critical role, as the compacted graphite form in the tested samples provides better support for the matrix, thereby enhancing the material's resistance to abrasive forces.

Machinability

Figure 6 presents the recorded data from the machinability test, showing the actual traverse curves of the cutting tool over time for all tested samples.

Our research indicates that the machinability of compacted graphite iron (CGI) with titanium (Ti) additions is comparable to

that of the base cast iron (without Ti) and reference samples of ferritic cast iron. Conversely, the angle of inclination of the machining curve for the pearlitic spheroidal graphite iron reference sample suggests inferior machinability. This implies that the analyzed samples from series I and III, with wall thicknesses of 5 mm and 13 mm, exhibit machinability similar to ferritic spheroidal graphite iron, and the applied titanium additions do not induce any significant changes in their machinability.

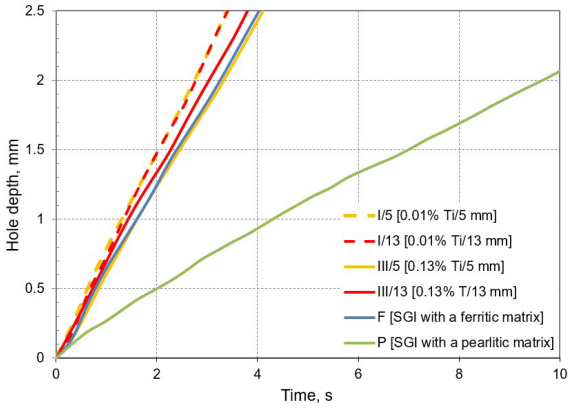

Fig. 6. Machinability Test Results
(I/5 – heat No. I, 5 mm wall thickness (based CGI);
I/13 – heat No. I, 13 mm wall thickness (based CGI);
III/5 – heat No. III, 5 mm wall thickness;
III/13 – heat No. III, 13 mm wall thickness;
F – spheroidal graphite iron with a ferritic matrix;
P – spheroidal graphite iron with a pearlitic matrix)

4. Conclusions

Based on the present study, the following conclusions can be drawn:

1. The introduction of titanium (Ti) in amounts up to 0.13% was found to be effective in controlling graphite morphology in thin-walled castings (≤ 5 mm), where high cooling rates often lead to excessive nodularity. This allows for achieving a high proportion of compacted (vermicular) graphite.
2. Despite the high cooling rates associated with thin-walled castings, a homogeneous, chill-free microstructure was consistently obtained. The addition of Ti promotes the formation of fine, homogeneously distributed precipitates, which were identified by EDS analysis as primarily titanium carbonitrides (Ti_2CN) and titanium carbides (TiC). These precipitates have a maximum size of less than 4 µm and a total volume fraction of less than 1%.
3. The results from this study indicate that the addition of titanium does not have a detrimental effect on the mechanical properties of the thin-walled compacted graphite iron (CGI) castings under the tested conditions. This suggests that the desirable structural and functional characteristics of these materials can be maintained even with Ti additions.

Acknowledgments

This research was conducted within Horizon Europe Project No. 101159771 — NetCastPL4.0.

References

[1] Dawson, S., Hollinger, I., Robbins, M., Daeth, J., Reuter, U. & Schultz, H. (2001). The effect of metallurgical variables on the machinability of compacted graphite iron. *SAE Transactions.* 110(5), 334-352.
[2] Behera, A., Mishra, S.C. (2012). New solution for property improvement of automobile parts. *Proceedings of Advances in Simulation & Optimization Techniques in Mechanical Engineering (NASOME-2012)*, 1-5.
[3] Guesser, W., Schroeder, T. & Dawson, S. (2001). Production Experience with compacted graphite iron automotive components. *AFS Transactions.* 109, 01-071, 1-11.
[4] Qiu, H. & Chen, Z. (2007). The forty years of vermicular graphite cast iron development in China (Part III). *China Foundry.* 4, 261-269.
[5] Liu, J. & Ding, N.X. (1985). Effect of type and amount of treatment alloy on compacted graphite produced by the Flotret process. *AFS Transactions.* 93, 675-688.
[6] Dawson, S. & Schroeder, T. (2004). Practical applications for compacted graphite iron. *AFS Transactions.* 47(5), 1-9.
[7] Charoenvilaisiri, S., Stefanescu, D.M., Ruxanda, R. & Piwonka, T.S. (2002). Thin wall compacted graphite iron castings. *AFS Transactions*. 2, 176, 1113-1130.
[8] Sofroni, L., Riposan, I., Chira, I. (1974). Some considerations on the crystallization features of cast irons with intermediate-shaped graphite (vermicular type). In *Proceedings of the 2nd International Symposium on the Metallurgy of Cast Iron*, Geneva, 1976 (pp. 179-196).
[9] Podrzucki, C., Wojtysiak, A. (1988). *Unalloyed ductile iron. Part II cast iron with vermicular graphite*. Cracow: AGH Ed.
[10] Górny, M. (2010). *Structure formation of ultra-thin wall ductile iron castings*. Cracow: Akapit Ed.
[11] Zhou, J. (2011). Vermicular graphite cast iron (I). *China Foundry*. 8(1), 154-164.
[12] Li, K., Zhang, X., Wang, Y. & Liu, J. (2024). Influence of cooling rate on microstructure and mechanical properties of thin-walled compacted graphite iron. *Journal of Materials Science & Technology.* 98, 200-208.
[13] Kowalski, M., Nowak, P. & Wójcik, A. (2024). Solidification behavior of thin-walled compacted graphite iron castings. *Archives of Metallurgy and Materials*. 69(2), 451-458.
[14] Riposan, I., Chisamera, M., Kelley, R., Barstow, M. & Naro, R.L. (2003). Magnesium-sulfur relationships in ductile and compacted graphite cast irons as influenced by late sulfur additions. *AFS Transactions*. 111(03-093), 869-883.
[15] Shy, Y., Hsu, C., Lee, S. & Hou, C. (2000). Effects of titanium addition and section size on microstructure and mechanical properties of compacted graphite cast iron.

Materials Science and Engineering A. 278(1-2), 54-60. https://doi.org/10.1016/S0921-5093(99)00599-7.
[16] Chen, Z., Li, X. & Wang, B. (2023). Role of titanium in controlling graphite morphology in compacted graphite iron. *International Journal of Cast Metals Research.* 36(3), 190-198.
[17] Nowak, A. & Olejnik, B. (2024). Thermal conductivity of compacted graphite iron: recent advances and future perspectives. *Archives of Foundry Engineering.* 24(1), 35-42.
[18] Zielinski, J. & Kowalczyk, M. (2024). Mechanical properties of compacted graphite iron under different cooling conditions. *Archives of Foundry Engineering.* 24(2), 112-120.
[19] Wróbel, P. & Szymański, A. (2024). Control of graphite morphology in compacted graphite iron: a review of recent developments. *Metallurgy and Foundry Engineering*. 50(1), 5-14.
[20] Nowak, K.J. & Wiśniewski, M. (2024). Influence of inoculation on microstructure and properties of thin-walled iron castings. *Metallurgy and Foundry Engineering*. 50(2), 121-130.
[21] Zeng, D., Zhang, Y., Liu, J., He, H. & Hong, X. (2008). Characterization of titanium–containing compounds in gray iron. *Tsinghua Science and Technology*. 13(2), 127-131. https://doi.org/10.1016/S1007-0214(08)70022-1.
[22] Myszka, D., Karwiński, A., Leśniewski, W. & Wieliczko, P. (2007). Influence of the type of ceramic moulding materials on the top layer of titanium precision castings. *Archives of Foundry Engineering*. 7(1), 153-156. ISSN (1897-3310).
[23] Górny, M., Kawalec, M., Sikora, G. & Lopez, H. (2014). Effect of cooling rate and titanium additions on microstructure of thin-walled compacted graphite iron castings. *ISIJ International*. 54(10), 2288-2293. https://doi.org/10.2355/isijinternational.54.2288.